Small-Animal SPECT/CT of HER2 and HER3 Expression in Tumor Xenografts in Athymic Mice Using Trastuzumab Fab–Heregulin Bispecific Radioimmunoconjugates

Eva J. Razumienko[1], Deborah A. Scollard[1], and Raymond M. Reilly[1–3]

[1]Department of Pharmaceutical Sciences, University of Toronto, Toronto, Ontario, Canada; [2]Department of Medical Imaging, University of Toronto, Toronto, Ontario, Canada; and [3]Toronto General Research Institute, University Health Network, Toronto, Ontario, Canada

Heterodimerization of human epidermal growth factor receptor 2 (HER2) with HER3 initiates aberrant downstream growth-signaling pathways in tumors. Our objective was to construct bispecific radioimmunoconjugates (bsRICs) that recognize HER2 and HER3 and evaluate their ability to image tumors in athymic mice that express one or both receptors using small-animal SPECT/CT. **Methods:** bsRICs were constructed by reacting the maleimide-derivatized trastuzumab Fab fragments that bind HER2 with a thiolated form of the HER3-binding peptide of heregulin-β1 (HRG) with or without a 12- or 24mer polyethylene glycol (PEG) spacer. bsRICs were derivatized with diethylenetriaminepentaacetic acid for labeling with ^{111}In. The ability of ^{111}In-bsRICs to bind HER2 or HER3 was determined in competition assays with unlabeled Fab or HRG on cells expressing one or both receptors. Tumor and normal-tissue uptake were examined in CD1 athymic mice bearing subcutaneous tumor xenografts that expressed HER2, HER3, or both receptors, with or without the preadministration of unlabeled Fab or HRG to determine the specificity of uptake. **Results:** Conjugation of Fab to HRG was confirmed by sodium dodecyl sulphate polyacrylamide gel electrophoresis–Western blot and size-exclusion high-performance liquid chromatography. Improved HER2 and HER3 binding and greater displacement of binding by competitors was found for ^{111}In-bsRICs that incorporated a PEG spacer, with the PEG_{24} spacer being optimal. The highest uptake of ^{111}In-bsRICs (7.8% ± 2.1% injected dose per gram [%ID/g]) in BT-474 human breast cancer xenografts (HER2-positive/HER3-positive) occurred at 48 h after injection. The preadministration of trastuzumab Fab decreased uptake in SK-OV-3 (HER2-positive/HER3-negative) human ovarian cancer xenografts from 7.0 ± 1.2 to 2.6 ± 1.5 %ID/g ($P < 0.001$). The preadministration of an excess of HRG decreased uptake in MDA-MB-468 (HER2-negative/HER3-positive) human breast cancer xenografts from 4.4 ± 0.9 to 2.6 ± 0.5 %ID/g ($P < 0.05$). All tumors were imaged by small-animal SPECT/CT. **Conclusion:** ^{111}In-bsRICs composed of trastuzumab Fab and HRG exhibited specific binding in vitro to tumor cells displaying HER2 or HER3 and were taken up specifically in vivo in tumors expressing one or both receptors, permitting tumor visualization by small-animal SPECT/CT. These agents could be useful for imaging heterodimerized HER2 and HER3 receptors because their bivalent properties may result in preferential binding to the heterodimerized forms. The approach may also be extended to constructing bsRICs for visualizing other peptide growth factor receptors.

Key Words: breast cancer; SPECT; ^{111}In; HER2; HER3

J Nucl Med 2012; 53:1943–1950
DOI: 10.2967/jnumed.112.106906

Approximately 30% of all breast cancers show an overexpression of human epidermal growth factor receptor 2 (HER2) as a result of gene amplification (*1*). This receptor is the target for trastuzumab (Herceptin; Roche), a therapeutic monoclonal antibody that binds to the extracellular domain. However, HER2 must homodimerize or heterodimerize with another receptor in the epidermal growth factor receptor family before a cellular signaling pathway can be initiated. Recent work has shown that the heterodimerization of HER2 with HER3, its preferred dimerization partner (*2*), has an important function in the growth of breast cancer, because this heterodimer functions as an oncogenic unit and is associated with a more aggressive phenotype (*3,4*). HER3 binds its preferred ligand, heregulin, which promotes recruitment of HER2 to the complex. There is no known ligand for HER2, but the receptor is locked in a dimerization-ready conformation. When the HER2–HER3 heterodimer forms, the intracellular kinase domains of the 2 receptors autophosphorylate their C-terminal ends, leading to activation of the phosphoinositide 3-kinase–Akt pathway. This pathway causes a cascade of signals that are involved in the regulation of cellular processes responsible for the proliferation of tumor cells and thus a more aggressive phenotype (*5*).

New classes of therapeutic drugs against breast cancer, known as HER dimerization inhibitors, are being developed and are intended to block HER2–HER3 heterodimerization. The most well-known example is the monoclonal antibody pertuzumab (Perjeta; Roche). Recent clinical trial data have

Received Mar. 31, 2012; revision accepted Jul. 24, 2012.
For correspondence or reprints contact: Raymond M. Reilly, Leslie Dan Faculty of Pharmacy, University of Toronto, 144 College St., Toronto, ON, Canada, M5S 3M2.
E-mail: raymond.reilly@utoronto.ca
Published online Oct. 24, 2012.

shown that pertuzumab, which blocks HER2 dimerization, in combination with trastuzumab and docetaxel significantly prolonged progression-free survival for HER2-positive metastatic breast cancer patients as compared with trastuzumab and docetaxel alone (*6*). Preclinically, agents that will directly target these HER2–HER3 heterodimers have also been reported, including bispecific antibodies and bispecific single-chain Fvs that recognize HER2 and HER3 and were developed as novel immunotherapeutics (*7,8*).

Our objective was to develop a novel bispecific radioimmunoconjugate (bsRIC) consisting of a domain capable of binding to HER2 covalently cross-linked to a ligand for HER3 that may be capable of selectively imaging HER2–HER3 heterodimers. There is great value in targeting HER2 and HER3, because HER3 is the preferential binding partner of HER2, and the heterodimer formed by these 2 receptors constitutes one of the most potent signaling pairs of the HER family (*9*). In addition, the 2 receptors have been shown to be frequently coexpressed in human breast cancer, and such coexpression is associated with a poor prognosis for patients (*10–12*).

Here, we show that by designing these bsRICs with flexible cross-linkers of varying lengths we can provide greater mobility to the individual components of the imaging probe, thus allowing it to better bind both receptors simultaneously. Our results show that such bsRICs are able to retain specificity for the individual receptors both in vitro and in vivo and show good tumor uptake in mouse xenograft models that express HER2, HER3, or both receptors. These properties render the bsRICs capable of interacting with and potentially imaging heterodimerized HER2–HER3 receptors.

MATERIALS AND METHODS

Tumor Cells

SK-OV-3 human ovarian carcinoma cells and MDA-MB-468 and BT-474 human breast cancer cells were purchased from the American Type Culture Collection. SK-OV-3 and MDA-MB-468 cells were cultured in RPMI 1640 medium (Sigma-Aldrich) supplemented with 10% fetal bovine serum (Invitrogen). BT-474 cells were cultured in Dulbecco modified Eagle medium supplemented with 10% fetal bovine serum. All cells were cultured under a 5% CO_2 atmosphere at 37°C. Cells were selected on the basis of their reported expression levels of HER2 or HER3; expression levels were confirmed through radioligand binding assays (*8,13*).

Preparation of ^{111}In-Diethylenetriaminepentaacetic Acid (DTPA)-Fab-Heregulin-β1 (HRG)

bsRICs were prepared by cross-linking trastuzumab Fab fragments (50 kDa) to human HRG (7.5 kDa; Peprotech) (*14*) using the reaction scheme shown in Supplemental Figure 1 (supplemental materials are available online only at http://jnm.snmjournals.org). Fab fragments were generated by digestion of trastuzumab IgG using immobilized papain (Pierce) and purified by centrifugal ultrafiltration on an Amicon Ultra Centrifugal Filter Unit with a 10-kDa-molecular-weight cutoff (Millipore), as previously described (*15*). A maleimide functional group was introduced onto Fab fragments by treatment with a 10-fold molar excess of succinimidyl 4-[*N*-maleimidomethyl] cyclohexane-1-carboxylate (sulfoSMCC; Pierce) or analogs containing polyethylene glycol (PEG) chains with either 12 or 24 repeating units (PEG_{12} or PEG_{24}) providing a spacer arm length of 5.34 or 9.52 nm (53.4 or 95.2 Å), respectively. Fab fragments at a concentration of 1 mg/mL were reacted with the appropriate linker in phosphate-buffered saline (PBS) (pH 7.2) with 5 mM ethylenediaminetetraacetic acid for 1 h at room temperature (RT). The reaction mixture was purified on a Sephadex G25 minicolumn (Sigma-Aldrich) eluted with PBS (pH 7.4). Primary amines on the HRG peptide were modified by reaction with a 10-fold molar excess of 2-iminothiolane HCl (Pierce) in PBS (pH 8.0) with 5 mM ethylenediaminetetraacetic acid for 1 h at RT to insert a free sulfhydryl group. The reaction mixture was purified on a polyacrylamide P6 minicolumn (Bio-Rad). Fab fragments were immediately reacted with a 2-fold molar excess of thiolated HRG and purified by ultrafiltration on a Microcon 30K device (Millipore). bsRICs were reacted with a 4-fold molar excess of DTPA dianhydride (Sigma-Aldrich) in 50 mM $NaHCO_3$ (pH 8.0) for 1 h at RT, and excess DTPA was removed on a Sephadex G25 minicolumn eluted with 1 M sodium acetate (pH 6.0). Both the thioether linkage used to cross-link thiolated heregulin to maleimide-derivatized trastuzumab Fab and the ^{111}In-DTPA complex have been shown to be stable (*16,17*). Purified DTPA-Fab-HRG was labeled with $^{111}InCl_3$ (MDS Nordion) for 1 h at RT. The final radiochemical purity was greater than 95% as measured by instant thin-layer silica gel chromatography (Pall Life Sciences) developed in sodium citrate (100 mM, pH 5.0).

Characterization of ^{111}In-DTPA-Fab-HRG

The successful conjugation of Fabs to HRGs and the purity of the bsRICs were assessed by Western blot and size-exclusion high-performance liquid chromatography (SE-HPLC). Sodium dodecyl sulphate polyacrylamide gel electrophoresis was performed on a 7.5% Tris-HCl minigel (Bio-Rad) under nonreducing conditions. Western blot was then performed by transferring electrophoresed proteins onto a polyvinylidene fluoride membrane (Bio-Rad). Membranes were probed with anti-HRG and anti-Fab antibodies as described in the supplemental information. Reactive bands were detected using the chromogenic substrate 3,3′-diaminobenzidine tetrahydrochloride (Sigma-Aldrich). To confirm conjugation to Fab, HRG was labeled with ^{111}In to be used as a radiotracer for SE-HPLC analysis. HRG was reacted with a 4-fold molar excess of DTPA dianhydride (Sigma-Aldrich) in 50 mM $NaHCO_3$ (pH 8.0) for 1 h at RT, and excess DTPA was removed on a polyacrylamide P6 minicolumn. Purified DTPA-HRG was labeled with $^{111}InCl_3$ for 1 h at RT. The final radiochemical purity was measured by instant thin-layer silica gel chromatography developed in sodium citrate (100 mM, pH 5.0). This radiotracer was then reacted with Traut's reagent as described above to introduce a free sulfhydryl group. Combinations of ^{111}In-HRG (without sulfhydryl) and Fab-SMCC or ^{111}In-HRG-sulfhydryl and Fab were reacted for 1 h at RT. SE-HPLC was performed on a BioSep SEC-S2000 column (Phenomenex) eluted with 100 mM NaH_2PO_4 buffer (pH 7.0) at a flow rate of 0.8 mL/min using a Series 200 pump (PerkinElmer) interfaced with a diode array detector (ultraviolet; PerkinElmer) set at 280 nm and a Radiomatic 610TR flow scintillation analyzer (PerkinElmer).

Competition Receptor Binding Assays

The ability of the bsRICs to bind to HER2 and HER3 was measured by competition binding assays using SK-OV-3 (HER2-positive [HER2+]), MDA-MB-468 (HER3-positive [HER3+]), and BT-474 (HER2+/HER3+) cells. Approximately 1.5×10^5 cells were

seeded into 24-well plates and cultured overnight. The medium was removed, and the cells were rinsed in cold PBS. The cells were then exposed to 10 nM (4.5 MBq/μg) ^{111}In-Fab-HRG, ^{111}In-Fab-PEG$_{12}$-HRG, or ^{111}In-Fab-PEG$_{24}$-HRG in PBS in the presence of 1,000 nM unlabeled Fab, HRG, or both for 1-point assays, or increasing concentrations (0–1,200 nM) of unlabeled Fab, HRG, or both for competition assays. Both assays were performed in a total volume of 500 μL of PBS for 3 h at 4°C to measure only cell-surface binding and prevent internalization of the radioimmunoconjugates (*15*). Unbound radioactivity was removed, and the cells were rinsed 2 times with PBS and then solubilized in 200 μL of 100 mM NaOH for 30 min at 37°C. The solubilized cells were transferred to γ-counting tubes, and the cell-bound radioactivity was measured in a γ-counter. For competition assays, the cell-bound ^{111}In-labeled bsRICs in the presence of competitor was normalized against cell-bound bsRICs in the absence of competitor (B/B_0) and plotted versus the logarithm of the competitor concentration (log C). The data were fitted to a 1-site competition model by Prism software (version 4.0; GraphPad Software), and the effective concentration that caused 50% displacement of the binding of the ^{111}In-labeled bsRICs to the cells (EC_{50}) was calculated.

SPECT/CT

Small-animal SPECT/CT was performed on female athymic CD1 *nu/nu* mice (Charles River) bearing subcutaneous BT-474 (HER2+/HER3+) tumor xenografts at 4, 24, 48, and 72 h after injection and in mice bearing subcutaneous SK-OV-3 and MDA-MB-468 tumor xenografts at 48 h after injection. For BT-474 xenografts, mice were inoculated with a 0.72-mg, 60-d sustained-release 17β-estradiol pellet (Innovative Research of America), and 48 h later the mice were inoculated subcutaneously in the thigh with 1×10^7 cells in 200 μL of a 1:1 mixture of Matrigel (BD Biosciences) and serum-free growth medium. For SK-OV-3 and MDA-MB-468 xenografts, mice were inoculated with 1×10^7 cells in 100 μL of serum-free growth medium. After 4–6 wk, groups of 3 mice with 200 ± 30 mm^3 tumors (measured with external calipers and calculated using length × width^2 × 0.5) were injected in the tail vein with ^{111}In-DTPA-Fab-PEG$_{24}$-HRG (10 μg, 35–40 MBq/mouse) in 100 μL of normal saline. For the blocking studies, 1 mg of unlabeled Fab or HRG was injected intraperitoneally 3 h before ^{111}In-DTPA-Fab-PEG$_{24}$-HRG injection. The tumor and normal-tissue uptake of ^{111}In-DTPA-Fab (10 μg, 35–40 MBq/mouse) and ^{111}In-DTPA-HRG (10 μg, 35–40 MBq/mouse) was also evaluated in SK-OV-3 and MDA-MB-468 xenografts, respectively. Mice were anesthetized by inhalation of 2% isoflurane in O_2. Imaging was performed on a NanoSPECT/CT tomograph (BioScan) equipped with 4 NaI(T1) detectors and fitted with 1.4-mm multipinhole collimators (full width at half maximum ≤ 1.2 mm). Twenty-four projections were obtained in a 256 × 256 acquisition matrix with a minimum of 90,000 counts per projection. Images were reconstructed using an ordered-subset expectation maximization algorithm (9 iterations). Cone-beam CT images were acquired (180 projections, 1 s/projection, 45 kVp) before small-animal SPECT images. Small-animal SPECT and CT images were coregistered using InVivoScope software (Bioscan).

Tumor and Normal-Tissue Uptake of bsRICs

Biodistribution studies were performed immediately after small-animal SPECT/CT. Mice were sacrificed and the tumor and samples of blood and selected normal tissues collected and weighed and their radioactivity counted in a γ-counter. Tumor and normal-tissue uptake were expressed as mean ± SD percentage injected dose per gram (%ID/g) and as tumor-to-blood and tumor-to-normal tissue ratios. The *Guide for the Care and Use of Laboratory Animals* (*18*) were followed, and all animal studies were conducted under a protocol (no. 989.1) approved by the Animal Care Committee at the University Health Network in accordance with the guidelines of the Canadian Council on Animal Care.

RESULTS

Synthesis and Characterization of bsRICs

The successful conjugation of Fab-HRG, Fab-PEG$_{12}$-HRG, and Fab-PEG$_{24}$-HRG was achieved (Supplemental Fig. 1). All immunoconjugates migrated on sodium dodecyl sulphate polyacrylamide gel electrophoresis under nonreducing conditions primarily as single bands (Supplemental Fig. 2A), with minor smearing observed, probably because of the PEG chains, which affected migration through the gel. Western blotting of all 3 immunoconjugates showed immunoreactivity of the bands with both anti-Fab and anti-HRG antibodies (Supplemental Fig. 2B), confirming conjugation. Increasing the PEG linker length caused an increase in overall estimated molecular weight between 60 and 65 kDa. Conjugation was further confirmed though the use of ^{111}In-HRG as a radiotracer for SE-HPLC analysis (Fig. 1A). A migration of the radioactivity peak from the HRG retention time of 13.0 min to the Fab retention time of 9.8 min was observed only when both components were modified with cross-linking agents. SE-HPLC analysis of Fab-HRG immunoconjugates showed major peaks with retention times of 9.9, 9.6, 9.3, and 9.0 min for Fab, Fab-HRG, Fab-PEG$_{12}$-HRG, and Fab-PEG$_{24}$-HRG, respectively (Fig. 1B).

Binding of ^{111}In-bsRICs In Vitro to Tumor Cells

The binding of ^{111}In-labeled Fab-HRG, Fab-PEG$_{12}$-HRG, and Fab-PEG$_{24}$-HRG to HER2 and HER3 was displaced by a 50-fold molar excess of unlabeled Fab, HRG, or both on cells that expressed only HER2 (SK-OV-3), HER3 (MDA-MB-468), or both HER2 and HER3 (BT-474). In 1-point binding assays, an overall increase in total binding (in the absence of competitor) of the bsRICs was observed when the length of the PEG chain was increased for cells expressing only HER2 (SK-OV-3) or HER3 (MDA-MB-486) (Fig. 2). In addition, insertion of a PEG spacer between Fab and HRG improved displacement of binding of ^{111}In-bispecific immunoconjugates (bsRICs) to HER2 and HER3 in BT-474 cells that express both receptors. For ^{111}In-bsRICs with the longest spacer (PEG$_{24}$), the binding to BT-474 cells (HER2+/HER3+) was reduced to 32.7% ± 0.3%, 51.2% ± 1.3%, and 15.0% ± 0.4%, respectively, by competition with trastuzumab Fab, HRG, or both ligands. The binding to SK-OV-3 cells (HER2+/HER3-negative [HER3−]) was reduced to 16.7% ± 0.8%, 88.8% ± 5.3%, or 13.4% ± 0.1% by trastuzumab Fab, HRG, or both ligands. The binding to MDA-MB-468 cells (HER2-negative [HER2−]/HER3+) was reduced to 98.5% ± 1.5%, 68.8% ± 0.3%, or 64.8% ± 4.5% by trastuzumab Fab, HRG, or both ligands. Less efficient competition for HER3 was observed for the PEG$_{12}$ spacer, and little competition for ^{111}In-bsRICs was observed

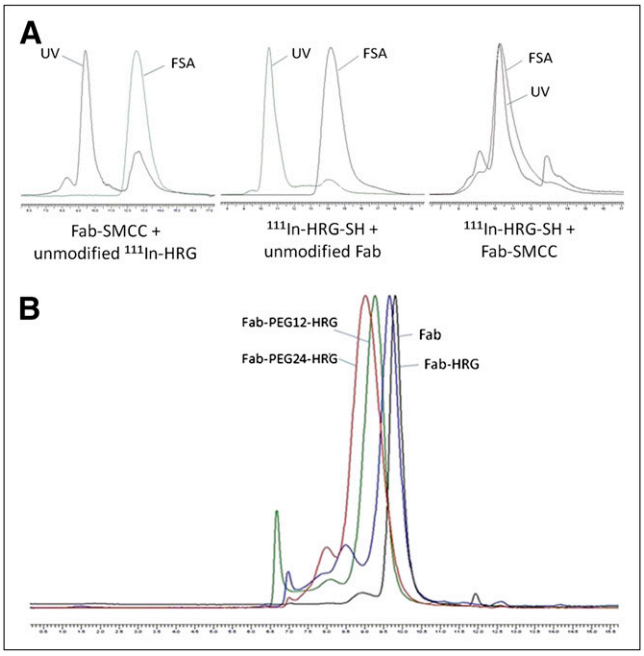

FIGURE 1. SE high-performance liquid chromatograms of bsRICs analyzed on BioSep-SEC-S2000 column eluted with 0.1 M NaH_2PO_4 (pH 7.0) at flow rate of 0.8 mL/min with ultraviolet detection at 280 nm and radioactivity (FSA) detection using a flow scintillation analyzer. (A) ^{111}In-HRG was used as radiotracer to confirm that conjugation occurred only when both Fab and HRG were modified with appropriate cross-linkers (SH = sulfhydryl; SMCC = succinimidyl 4-{N-maleimidomethyl}cyclohexane-1-carboxylate). (B) Ultraviolet trace of all bsRICs. Fab was eluted at retention time of 9.9 min. Peaks at earlier retention times represent higher-molecular-weight aggregates (<10%). Retention time gradually decreased with increasing PEG linkers. FSA= flow scintillation analyzer; SH = sulfhydryl; SMCC = succinimidyl 4-{N-maleimidomethyl}cyclohexane-1-carboxylate; UV = ultraviolet.

without a PEG spacer. To examine HER2 or HER3 binding of the ^{111}In-bsRICs with a PEG_{24} spacer in more detail, competition binding curves were obtained with displacement of radioligand binding by increasing concentrations of trastuzumab Fab or HRG (Fig. 3). Fitting of the curves to a 1-site-competition binding model estimated that the EC_{50} values were 9.1 and 6.7 nM with Fab on BT-474 and SK-OV3 cells, respectively, and 41.1 and 32.7 nM with HRG on BT-474 and MDA-MB-468 cells, respectively. These assays were also performed using ^{111}In-DTPA-Fab and ^{111}In-DTPA-HRG, which had EC_{50} values of 1.4 and 21.3 nM, respectively, on BT-474 cells (not shown). Even at the highest concentrations of HRG, it was not possible to completely displace the binding of the bsRICs to HER3 on MDA-MB-468 cells. Because of its optimal HER2 and HER3 binding properties, ^{111}In-DTPA-Fab-PEG_{24}-HRG was selected for tumor imaging studies in vivo.

Uptake of ^{111}In-bsRICs and Micro-SPECT/CT In Vivo

Small-animal SPECT/CT images of ^{111}In-DTPA-Fab-PEG_{24}-HRG in mice bearing BT-474 (HER2+/HER3+) xenografts showed accumulation in the tumor and low normal-tissue uptake at 24, 48, and 72 h after injection (Fig. 4), with the exception of the kidneys. Maximum tumor uptake was seen at 48 h after injection and was confirmed by biodistribution studies that showed an uptake of 7.8 ± 2.1 %ID/g and a tumor-to-blood ratio of 11.1 ± 2.9 (Supplemental Table 1). The uptake of ^{111}In-DTPA-Fab-PEG_{24}-HRG was then examined in mice with SK-OV-3 (HER2+/HER3−) and MDA-MB-468 (HER2−/HER3+) tumors at 48 h after injection. Tumor uptake was seen in both xenografts on small-animal SPECT/CT images (Fig. 5) and confirmed in biodistribution studies (Table 2). When preadministered an excess of Fab, ^{111}In-DTPA-Fab-PEG_{24}-HRG uptake in SK-OV-3 tumors was significantly decreased (2.6-fold, from 7.0 ± 1.2 %ID/g to 2.6 ± 1.5 %ID/g, $P < 0.001$). Uptake of ^{111}In-DTPA-Fab-PEG_{24}-HRG significantly decreased 1.6-fold in MDA-MB-468 xenografts (from 4.4 ± 0.9 %ID/g to 2.6 ± 0.5 %ID/g, $P < 0.05$) when these mice were preadministered an excess of HRG. These decreases confirm that the tumor uptake of these bsRICs was specific. Tumor uptake was observed for ^{111}In-DTPA-Fab in SK-OV-3 xenografts (7.9 ± 1.4 %ID/g); however, low uptake was found for ^{111}In-DTPA-HRG in MDA-MB-468 xenografts (2.1 ± 0.4 %ID/g) (Table 3).

DISCUSSION

bsICs provide a unique opportunity to specifically probe 2 antigens. For example, bsICs have been formed from single-chain Fv fragments of antibodies for the enhancement of antigen-specific immune recognition of cancer cells, allowing

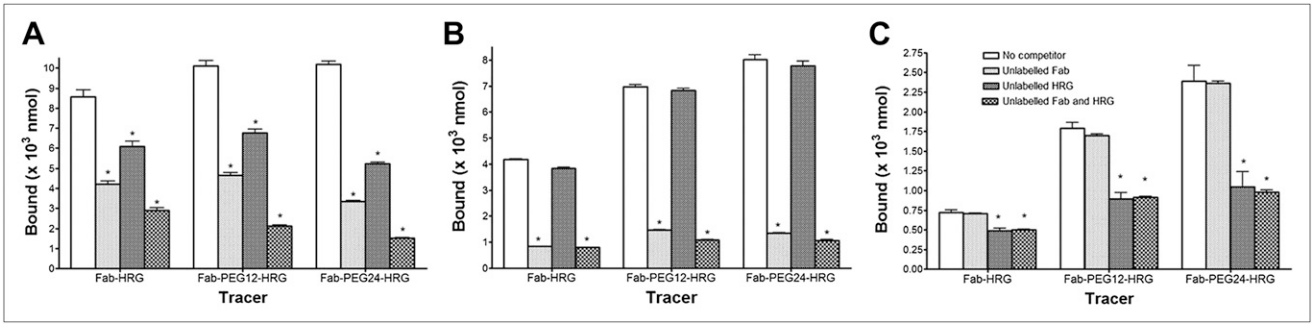

FIGURE 2. Binding of ^{111}In-labeled bsRICs to HER2 and HER3 on tumor cells in 1-point competition binding assays using 10 nM ^{111}In-Fab-HRG, ^{111}In-Fab-PEG_{12}-HRG, or ^{111}In-Fab-PEG_{24}-HRG alone or competed with 50-fold molar excess of unlabeled trastuzumab Fab, HRG, or both in cell lines that are HER2+/HER3+ (BT-474) (A), HER2+/HER3− (SK-OV-3) (B), or HER2−/HER3+ (MDA-MB-468) (C).

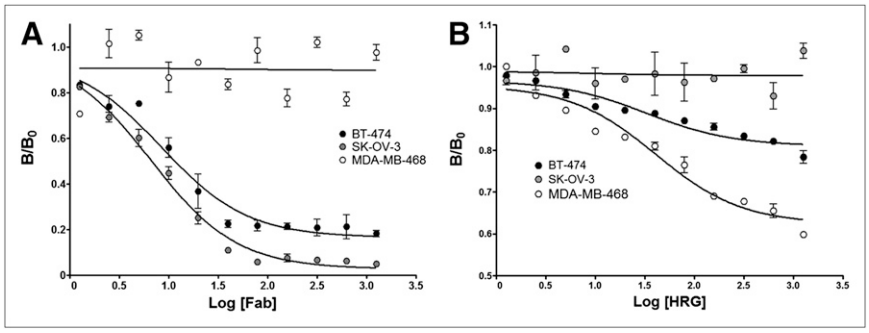

FIGURE 3. Displacement of binding of 10 nM ^{111}In-Fab-PEG$_{24}$-HRG bsRICs to HER2 and HER3 by increasing concentrations of trastuzumab Fab (A) and HRG (B) in cell lines that are HER2+/HER3+ (BT-474), HER2+/HER3− (SK-OV-3), or HER2−/HER3+ (MDA-MB-468). By fitting curves to 1-site competition binding model, EC_{50} values were estimated to be 9.1 and 6.7 nM with Fab on BT-474 and SK-OV3 cells and 41.1 and 32.7 nM with HRG on BT-474 and MDA-MB-468 cells, respectively.

for a better targeted delivery of cytotoxic agents (*8*). Another bispecific antibody against HER2–HER3 inhibited HER3 signaling and demonstrated antitumor activity in preclinical models that are dependent on HER2 overexpression (*7*). In nuclear medicine bsICs have been widely investigated as pretargeting agents, with the ability to bind a tumor-associated antigen and a radionuclide carrier, allowing for faster imaging after injection and lower exposure of normal tissues to radioactivity (*19,20*). In this study, we report for the first time, to our knowledge, the preparation, characterization, and receptor binding properties of ^{111}In-labeled bsRICs capable of binding both HER2 and HER3. We further examined their tumor and normal-tissue localization and showed their specificity for these receptors through in vivo blocking studies. We hypothesized that such probes may be able to differentiate heterodimers from monomeric receptors because of stronger bivalent binding and avidity for the dimers as opposed to monovalent binding to the individual HERs (*21*). In addition, heterodimerization of HER2 and HER3 results in a conformational change that produces a complex that binds HRG (the HER3 ligand) more strongly than the HER3 receptor alone (*22*). Because the HER3 binding domain of HRG was incorporated into the bsRICs, this may encourage high-affinity binding to heterodimerized HER2–HER3 complexes. Finally, although the density of HER3 on cells is much lower than that of HER2, it has been shown to cluster with HER2 on lipid rafts, promoting HER2–HER3 heterodimerization and possibly increased binding of the bsRICs to heterodimers (*23*).

The bsICs described here were composed of a Fab fragment of trastuzumab cross-linked to the epidermal growth factor–like domain of HRG, the endogenous ligand for HER3 (Supplemental Fig. 1). To examine the effects of steric hindrance on the ability to bind HER2 and HER3, various-length PEG spacers (12- and 24mer) were incorporated. Western blot analysis confirmed conjugation by probing with antibodies specific for the Fab or HRG components of the bsICs. In addition, the upward band shift corresponded to the increase in size expected with incorporation of longer PEG chains (Supplemental Fig. 2). These results were confirmed by SE-HPLC, using HRG labeled with ^{111}In in trace amounts incorporated into the reaction, which showed conjugation only when both Fab and HRG were modified with cross-linkers (Fig. 1).

The incorporation of the PEG spacers improved the receptor binding capabilities of each component (trastuzumab Fab or HRG; Fig. 2). Incorporation of longer PEG chains improved overall receptor binding of the bsRICs but also provided greater displacement of binding by an excess of unlabeled Fab or HRG in cells that expressed HER2 (SK-OV-3), HER3 (MDA-MB-468), or both receptors (BT-474), with the

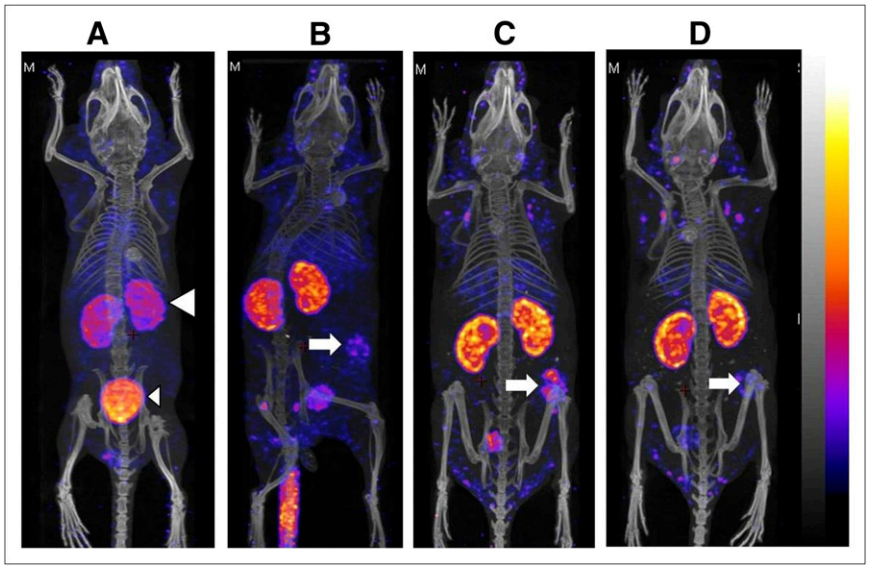

FIGURE 4. Posterior whole-body small-animal SPECT/CT images of female CD1 athymic mice implanted subcutaneously in right hind flank with HER2+/HER3+ BT-474 human breast cancer xenografts at 4 (A), 24 (B), 48 (C), and 72 h (D) after injection of ^{111}In-Fab-PEG$_{24}$-HRG. Tumor xenografts (arrows) were visualized in B–D but not in A. Also visualized are kidneys (large arrowhead) and bladder (small arrowhead).

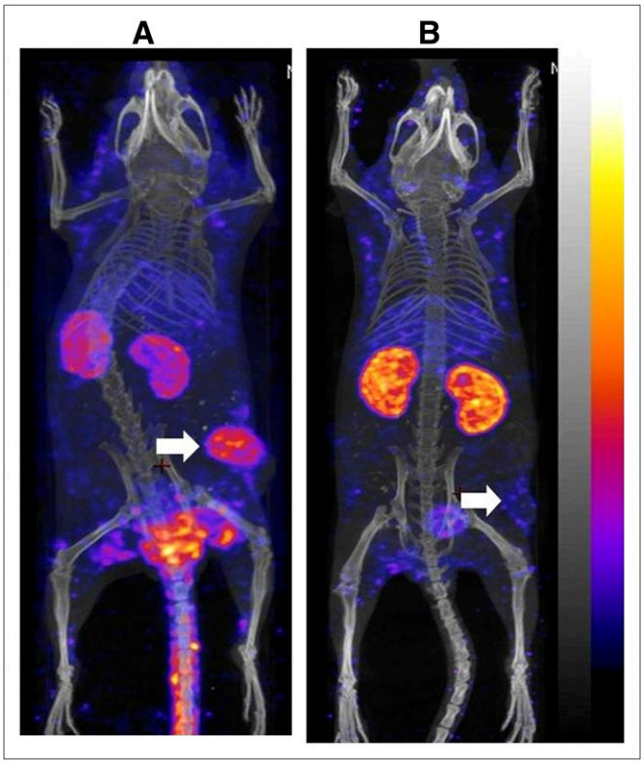

FIGURE 5. Posterior whole-body small-animal SPECT/CT images of female CD1 athymic mice implanted subcutaneously in right hind flank with SK-OV-3 (HER2+) human ovarian cancer xenografts (A) or MDA-MB-468 (HER3+) human breast cancer xenografts (arrows) (B) at 48 h after intravenous tail injection of ^{111}In-Fab-PEG$_{24}$-HRG.

optimal properties displayed by ^{111}In-DTPA-Fab-PEG$_{24}$-HRG. Displacement by HRG was not obtained in SK-OV-3 cells that were HER2+/HER3−. Similarly, trastuzumab Fab did not displace binding of these bsRICs to HER2−/HER3+ MDA-MB-468 cells. The apparently poor ability to completely displace binding of the bsRICs to MDA-MB-48 cells was likely due to the low HER3 density (~35,000 receptors per cell). Because of the low HER3 density, this results in a lower total amount of bsRICs bound, which—combined with a similar amount of nonspecific binding (i.e., not displaceable by HRG)—provides a lower proportion of specific (displaceable) binding. In the case of BT-474 cells that express both HER2 and HER3, the total binding of the bsRICs was displaced to 32.7% ± 0.3% by unlabeled Fab, 51.2% ± 1.3% by unlabeled HRG, and 15.0% ± 0.4% by Fab combined with HRG. The reason for the residual binding of the bsRICs to BT-474 cells when competed with HRG and Fab is not known but may be due to the high avidity bispecific binding to the heterodimerized receptors that is not easily displaced by either ligand.

When competition assays for ^{111}In-DTPA-Fab-PEG$_{24}$-HRG were performed over a range of Fab and HRG concentrations (Fig. 3), the observed EC_{50} values were 9.1 and 6.7 nM with Fab on BT-474 and SK-OV-3 cells, respectively, and 41.1 and 32.7 nM with HRG on BT-474 and MDA-MB-468 cells, respectively. In cells that express both HER2 and HER3, the overall higher displacement of ^{111}In-DTPA-Fab-PEG$_{24}$-HRG by both ligands, compared with displacement when treated with only Fab or HRG, suggests that there may be some residual binding of the RICs as a result of interaction with heterodimerized receptors that cannot be displaced by a single competitor. This possibility may also explain why higher concentrations of individual competitors were necessary to displace the binding of ^{111}In-DTPA-Fab-PEG$_{24}$-HRG to BT-474 cells that express both HER2 and HER3 as opposed to SK-OV-3 or MDA-MB-468 cells that display only HER2 or HER3, respectively.

Because of its favorable properties in vitro, ^{111}In-DTPA-Fab-PEG$_{24}$-HRG was selected for further study in vivo in tumor-bearing mice. Optimal imaging conditions were first determined in mice implanted subcutaneously with BT-474 tumors, which are positive for both HER2 and HER3. Mice were imaged at 4, 24, 48, and 72 h after injection of bsRICs. Tumor uptake was not seen at 4 h but was observed at all time points after 24 h, with the highest uptake and tumor-to-blood ratio found at 48 h (Table 1). These results are similar to those previously reported for ^{111}In-labeled trastuzumab Fab fragments by our group, which revealed a tumor uptake of 8.4 ± 1.8 %ID/g at 48 h after injection in BT-474 tumor xenografts (*15*). Pharmacokinetic elimination of ^{111}In-DTPA-Fab-PEG$_{24}$-HRG from the blood was consistent with ^{111}In-DTPA-trastuzumab Fab (0.7 ± 0.1 %ID/g vs. 0.9 ± 0.3 %ID/g at 48 h after injection) but differed from ^{111}In-DTPA-trastuzumab IgG, which exhibited a blood concentration of 3.5 ± 1.0 %ID/g at 72 h after injection in mice with MDA-MB-361 tumor xenografts (*24*). Using this time point, we further examined the in vivo properties of ^{111}In-DTPA-Fab-PEG$_{24}$-HRG, including its ability to bind HER2 and HER3 in mice bearing subcutaneous SK-OV-3 and MDA-MB-468 xenografts, respectively. To confirm specificity for these target receptors, blocking studies were performed by preadministering an excess of Fab or HRG. In the case of SK-OV-3 xenografts, Fab blocking caused a significant 2.6-fold decrease in tumor uptake, whereas in MDA-MB-468 xenografts a significant 1.6-fold decrease was noted with HRG preadministration (Table 2). Uptake in all other tissues remained unchanged with and without blocking. These results demonstrated that ^{111}In-DTPA-Fab-PEG$_{24}$-HRG bound specifically to both HER2 and HER3 in vivo.

For comparison, the tumor and normal-tissue uptake of ^{111}In-DTPA-Fab in mice with SK-OV-3 xenografts and ^{111}In-DTPA-HRG in mice with MDA-MB-468 xenografts was examined at this same time point (Table 3). Although the uptake of ^{111}In-DTPA-Fab in SK-OV-3 xenografts was comparable to that of the bsRIC, much lower tumor uptake was observed with ^{111}In-DTPA-HRG in MDA-MB-468 xenografts, possibly because of the rapid elimination of ^{111}In-DTPA-HRG from the blood. To our knowledge, this is the first time uptake of radiolabeled HRG into tumors expressing HER3 has been reported. As such, the bsRIC may provide imaging of HER3 expression in tumors better than that using ^{111}In-DTPA-HRG. We were not able to image MDA-MB-468 xenografts using ^{111}In-DTPA-HRG (results not shown).

TABLE 1
Tumor and Normal-Tissue Uptake of ^{111}In-DTPA-Fab-PEG$_{24}$-HRG in BT474 Tumor Xenografts at Selected Times

Tissue	%ID/g			
	4 h	24 h	48 h	72 h
Blood	7.4 ± 0.8	1.1 ± 1.0	0.7 ± 0.1	0.5 ± 0.1
Heart	2.3 ± 0.3	1.1 ± 0.3	0.9 ± 0.2	0.7 ± 0.2
Lung	2.4 ± 0.4	1.0 ± 0.5	0.6 ± 0.1	0.7 ± 0.1
Liver	1.2 ± 0.2	1.7 ± 0.5	1.8 ± 0.1	2.4 ± 0.6
Kidney	2.7 ± 0.2	4.5 ± 1.0	6.4 ± 0.7	8.6 ± 0.8
Spleen	1.6 ± 0.3	1.7 ± 0.4	1.9 ± 0.3	1.9 ± 0.3
Stomach	1.4 ± 0.2	0.7 ± 0.2	0.5 ± 0.1	0.5 ± 0.3
Small intestines	1.2 ± 0.3	0.9 ± 0.3	0.7 ± 0.1	0.6 ± 0.2
Large intestines	1.6 ± 0.5	0.8 ± 0.1	0.6 ± 0.1	0.7 ± 0.3
Muscle	0.6 ± 0.2	0.5 ± 0.1	0.4 ± 0.2	0.2 ± 0.1
Tumor	1.7 ± 0.9	5.4 ± 2.2	7.8 ± 2.1*	4.1 ± 2.5
Bladder	2.3 ± 1.2	1.4 ± 0.3	2.0 ± 0.1	1.9 ± 0.6
Skin	1.5 ± 0.4	2.2 ± 0.8	1.5 ± 0.9	1.2 ± 0.4
Tail	2.0 ± 0.4	1.0 ± 0.1	0.8 ± 0.1	0.8 ± 0.3

*Significantly higher than at other time points ($P < 0.05$).

CD1 athymic mice with HER2+/HER3+ BT-474 xenografts were administered 35–40 MBq/10 μg of ^{111}In-DTPA-Fab-PEG$_{24}$-HRG ($n = 4$), and tissue distribution was determined at selected time points after intravenous (tail vein) injection. Data are mean ± SD.

Here, we have described the construction of a bsRIC that recognizes both HER2 and HER3, an important prerequisite for an imaging agent that might ultimately detect HER2–HER3 heterodimers. Our results show that these bsRICs bind in higher amounts and more strongly to cells that express both HER2 and HER3 than to cells that express only 1 of these receptors. We are now exploring methods to discriminate the binding of the bsRICs to heterodimerized receptors using inhibitors such as pertuzumab, which can diminish their binding (*25*), and assess the extent of heterodimerization in the tumor cells using various techniques (*22*). Should these studies prove promising, the ability of the bsRICs to differentiate between tumors with low or high levels of heterodimerized HER2–HER3 receptors will be studied by imaging.

TABLE 2
Tumor and Normal-Tissue Uptake of ^{111}In-DTPA-Fab-PEG$_{24}$-HRG in SK-OV-3 and MDA-MB-468 Xenografts

Tissue	%ID/g			
	SK-OV-3 (HER2+)		MDA-MB-468 (HER3+)	
	Unblocked	Blocked*	Unblocked	Blocked*
Blood	0.7 ± 0.1	1.2 ± 0.1	0.7 ± 1.3	0.7 ± 0.1
Heart	0.6 ± 0.1	1.6 ± 0.8	0.9 ± 0.3	0.7 ± 0.1
Lung	0.6 ± 0.1	1.4 ± 0.4	1.1 ± 0.8	0.6 ± 0.1
Liver	1.8 ± 0.5	1.4 ± 0.3	1.3 ± 0.9	1.8 ± 0.3
Kidney	5.4 ± 1.0	6.5 ± 1.4	7.2 ± 2.6	5.9 ± 0.8
Spleen	0.9 ± 0.3	1.9 ± 1.4	1.3 ± 0.8	1.4 ± 0.3
Stomach	0.4 ± 0.1	1.3 ± 0.4	0.4 ± 0.4	0.5 ± 0.1
Small intestines	0.5 ± 0.1	1.3 ± 0.9	1.0 ± 0.6	0.6 ± 0.1
Large intestines	0.3 ± 0.1	0.7 ± 0.5	0.9 ± 0.8	0.5 ± 0.1
Muscle	0.2 ± 0.1	1.1 ± 0.9	1.2 ± 0.4	0.3 ± 0.2
Tumor	7.0 ± 1.2	2.6 ± 1.5†	4.4 ± 0.9	2.6 ± 0.5‡
Bladder	0.6 ± 0.3	1.8 ± 0.5	1.6 ± 0.8	1.3 ± 0.2
Skin	1.5 ± 0.4	0.7 ± 0.4	1.5 ± 0.4	1.5 ± 0.6
Tail	0.4 ± 0.1	1.7 ± 0.6	1.3 ± 0.8	0.6 ± 0.1

*To block HER2 or HER3 on tumors, mice were preadministered excess of unlabeled trastuzumab Fab (1 mg) or unlabeled HRG (1 mg), respectively, by intraperitoneal injection 3 h before ^{111}In-DTPA-Fab-PEG$_{24}$-HRG injection.

†Significant difference from unblocked ($P < 0.001$).

‡Significant difference from unblocked ($P < 0.05$).

CD1 athymic mice were administered 35–40 MBq/10 μg of ^{111}In-DTPA-Fab-PEG$_{24}$-HRG ($n = 4$) and sacrificed at 48 h after injection. Data are mean ± SD.

TABLE 3
Tumor and Normal-Tissue Uptake of ^{111}In-DTPA-Fab in SK-OV-3 Xenografts and ^{111}In-DTPA-HRG in Mice with MDA-MB-468 Xenografts

Tissue	%ID/g	
	^{111}In-DTPA-HRG in MDA-MB-468 (HER3+)	^{111}In-DTPA-Fab in SK-OV-3 (HER2+)
Blood	0.3 ± 0.1	1.0 ± 0.1
Heart	0.5 ± 0.1	1.4 ± 0.1
Lung	0.6 ± 0.3	1.6 ± 0.5
Liver	1.1 ± 0.8	2.5 ± 0.4
Kidney	7.1 ± 2.1	6.0 ± 2.0
Spleen	1.3 ± 0.2	1.4 ± 3.1
Stomach	1.0 ± 0.2	1.4 ± 0.1
Small intestines	1.5 ± 0.3	0.8 ± 0.1
Large intestines	1.5 ± 0.2	0.7 ± 0.1
Muscle	0.9 ± 0.1	0.7 ± 0.1
Tumor	2.1 ± 0.4	7.9 ± 1.5
Bladder	1.2 ± 1.8	0.2 ± 0.2
Skin	1.0 ± 0.3	0.3 ± 0.2
Tail	1.7 ± 1.1	0.6 ± 0.2

CD1 athymic mice were administered 35–40 MBq/10 μg of ^{111}In-DTPA-Fab-PEG$_{24}$-HRG (n = 3) and sacrificed at 48 h after injection. Data are mean ± SD.

CONCLUSION

^{111}In-labeled bsRICs are composed of trastuzumab Fab fragments conjugated to the epidermal growth factor–like domain of HRG through a PEG spacer of appropriate length bound specifically to both HER2 and HER3. Examination of these bsRICs in athymic mice bearing tumor xenografts expressing HER2 or HER3 or both receptors showed good tumor uptake and low normal-tissue accumulation, with the exception of the kidneys. The optimal time point for small-animal SPECT/CT was at 48 h after injection. Blocking studies in mice with tumors expressing only HER2 or HER3 demonstrated the specificity for both receptors in vivo. The design and approach for synthesis of these bsRICs recognizing HER2 or HER3 could be applied to the construction of other bsRICs that bind to more than one peptide growth factor receptor.

DISCLOSURE STATEMENT

The costs of publication of this article were defrayed in part by the payment of page charges. Therefore, and solely to indicate this fact, this article is hereby marked "advertisement" in accordance with 18 USC section 1734.

ACKNOWLEDGMENTS

This research was supported by a grant from the Ontario Institute for Cancer Research (Smarter Imaging Program) with funds from the Province of Ontario and a Canadian Breast Cancer Foundation Doctoral Fellowship (Ontario region). Parts of this research were presented at the 101st Annual Meeting of the American Association of Cancer Research, Washington, D.C., April 17–21, 2011. No other potential conflict of interest relevant to this article was reported.

REFERENCES

1. Pauletti G, Dandekar S, Rong H, et al. Assessment of methods for tissue-based detection of the HER-2/neu alteration in human breast cancer: a direct comparison of fluorescence in situ hybridization and immunohistochemistry. *J Clin Oncol.* 2000;18:3651–3664.
2. Graus-Porta D, Beerli RR, Daly JM, Hynes NE. ErbB-2, the preferred heterodimerization partner of all ErbB receptors, is a mediator of lateral signaling. *EMBO J.* 1997;16:1647–1655.
3. Holbro T, Beerli RR, Maurer F, Koziczak M, Barbas CF 3rd, Hynes NE. The ErbB2/ErbB3 heterodimer functions as an oncogenic unit: ErbB2 requires ErbB3 to drive breast tumor cell proliferation. *Proc Natl Acad Sci USA.* 2003;100:8933–8938.
4. Alimandi M, Romano A, Curia MC, et al. Cooperative signaling of ErbB3 and ErbB2 in neoplastic transformation and human mammary carcinomas. *Oncogene.* 1995;10:1813–1821.
5. Pinkas-Kramarski R, Soussan L, Waterman H, et al. Diversification of Neu differentiation factor and epidermal growth factor signaling by combinatorial receptor interactions. *EMBO J.* 1996;15:2452–2467.
6. Baselga J, Cortes J, Kim SB, et al. Pertuzumab plus trastuzumab plus docetaxel for metastatic breast cancer. *N Engl J Med.* 2012;366:109–119.
7. McDonagh CF, Huhalov A, Harms BD, et al. Antitumor activity of a novel bispecific antibody that targets the ErbB2/ErbB3 oncogenic unit and inhibits heregulin-induced activation of ErbB3. *Mol Cancer Ther.* 2012;11:582–593.
8. Robinson MK, Hodge KM, Horak E, et al. Targeting ErbB2 and ErbB3 with a bispecific single-chain Fv enhances targeting selectivity and induces a therapeutic effect in vitro. *Br J Cancer.* 2008;99:1415–1425.
9. Tzahar E, Waterman H, Chen X, et al. A hierarchical network of interreceptor interactions determines signal transduction by Neu differentiation factor/neuregulin and epidermal growth factor. *Mol Cell Biol.* 1996;16:5276–5287.
10. Siegel PM, Ryan ED, Cardiff RD, Muller WJ. Elevated expression of activated forms of Neu/ErbB-2 and ErbB-3 are involved in the induction of mammary tumors in transgenic mice: implications for human breast cancer. *EMBO J.* 1999;18:2149–2164.
11. Travis A, Pinder SE, Robertson JF, et al. C-erbB-3 in human breast carcinoma: expression and relation to prognosis and established prognostic indicators. *Br J Cancer.* 1996;74:229–233.
12. Naidu R, Yadav M, Nair S, Kutty MK. Expression of c-erbB3 protein in primary breast carcinomas. *Br J Cancer.* 1998;78:1385–1390.
13. deFazio A, Chiew YE, Sini RL, Janes PW, Sutherland RL. Expression of c-erbB receptors, heregulin and oestrogen receptor in human breast cell lines. *Int J Cancer.* 2000;87:487–498.
14. Barbacci EG, Guarino BC, Stroh JG, et al. The structural basis for the specificity of epidermal growth factor and heregulin binding. *J Biol Chem.* 1995;270:9585–9589.
15. Tang Y, Wang J, Scollard DA, et al. Imaging of HER2/neu-positive BT-474 human breast cancer xenografts in athymic mice using ^{111}In-trastuzumab (Herceptin) Fab fragments. *Nucl Med Biol.* 2005;32:51–58.
16. Reilly RM. The radiopharmaceutical science of monoclonal antibodies and peptides for imaging and targeted in situ radiotherapy of malignancies. In: Gad SC, ed. *Handbook of Biopharmaceutical Technology.* Toronto, Canada: John Wiley & Sons; 2007:987–1053.
17. Shen BQ, Xu K, Liu L, et al. Conjugation site modulates the in vivo stability and therapeutic activity of antibody-drug conjugates. *Nat Biotechnol.* 2012;30:184–189.
18. *Guide for the Care and Use of Laboratory Animals*. Washington, DC: Government Printing Office; 1985. NIH publication 86-23.
19. Sharkey RM, Rossi EA, McBride WJ, Chang CH, Goldenberg DM. Recombinant bispecific monoclonal antibodies prepared by the dock-and-lock strategy for pretargeted radioimmunotherapy. *Semin Nucl Med.* 2010;40:190–203.
20. Schoffelen R, van der Graaf WT, Sharkey RM, et al. Pretargeted immuno-PET of CEA-expressing intraperitoneal human colonic tumor xenografts: a new sensitive detection method. *EJNMMI Res.* 2012;2:5.
21. Rudnick SI, Adams GP. Affinity and avidity in antibody-based tumor targeting. *Cancer Biother Radiopharm.* 2009;24:155–161.
22. Sliwkowski MX, Schaefer G, Akita RW, et al. Coexpression of erbB2 and erbB3 proteins reconstitutes a high affinity receptor for heregulin. *J Biol Chem.* 1994;269:14661–14665.
23. Nagy P, Vereb G, Sebestyen Z, et al. Lipid rafts and the local density of ErbB proteins influence the biological role of homo- and heteroassociations of ErbB2. *J Cell Sci.* 2002;115:4251–4262.
24. McLarty K, Cornelissen B, Scollard DA, Done SJ, Chun K, Reilly RM. Associations between the uptake of ^{111}In-DTPA-trastuzumab, HER2 density and response to trastuzumab (Herceptin) in athymic mice bearing subcutaneous human tumour xenografts. *Eur J Nucl Med Mol Imaging.* 2009;36:81–93.
25. Adams CW, Allison DE, Flagella K, et al. Humanization of a recombinant monoclonal antibody to produce a therapeutic HER dimerization inhibitor, pertuzumab. *Cancer Immunol Immunother.* 2006;55:717–727.